Some Features of the Western Tropical Pacific: Surface Wind Field and its Influence on the Upper Ocean Thermal Structure

Bingrong XU

Second Institute of Oceanography, SOA
Hangzhou, Zhejiang 310012
People's Republic of China

1. Introduction

Wyrtki (1974) and Meyers (1982) have indicated that the seasonal variation of the thermocline depth and the sea level in the tropical Pacific Ocean, which can represent the strength of major oceanic currents, are strongly influenced by the position of the trade wind. Affected by the East Asian Monsoon, sea surface wind field has apparently seasonal displacements in the western tropical Pacific. It appears that the position of the Inter-Tropical Convergence Zone of the wind (ITCZ) has large seasonal oscillation from about 15°S (February-March) to 10°N (September-October) as shown in Donguy et al (1982). Responding to the seasonal oscillation of the ITCZ, some oceanic thermal elements may have corresponding seasonal variations. Recently some research works, e.g. Donguy et al. (1982) and White et al. (1985), showed the sea surface wind field and the upper ocean thermal structure in the western tropical Pacific have interannual variations corresponding with El Nino-Southern Oscillation phenomenon (ENSO). Usually, anomalies of the wind field are leading ENSO by several months. Due to a lack of wind field and subsurface temperature data sets, the effects of surface wind field seasonal variations on the upper ocean thermal structure have not been clearly described in the western tropical Pacific.

In this study, seasonal and interannual variations of sea the surface wind field over the western tropical Pacific are described, using mean monthly sea surface pseudo wind stress data series from Jan. 1962 to Jan. 1980, and mean seasonal subsurface temperature data series from spring 1964 to winter 1980 (kindly provided by W. White and sea-air interaction group, Second Institute of Oceanography, SOA). The effects of the wind field on the upper ocean thermal structure are primarily analyzed.

2. Seasonal and interannual variations of the sea surface wind field

a. Seasonal variations.

The long-term monthly mean (1964-1980) zonal and meridional components of pseudo wind stress along 155°E are shown in Fig.1a-b. The zonal and meridional components of pseudo wind stress are represented by

$$\tau^x = u\,(u^2+v^2)^{1/2}; \qquad \tau^y = v\,(u^2+v^2)^{1/2} \tag{1}$$

where u and v, are the surface wind velocity components. From these figures it is apparent that the northeast and southeast trade winds are stronger in February to March and August to September respectively. The interface of the opposite zonal and meridional wind components may indicate the mean position of the ITCZ. The dashed line in Fig. 1 is the interface of the wind components and show that the mean position of the ITCZ is near 13°S during January to February and near 10°N during August to September, i.e., consistent with the indication of Donguy et al. (1982).

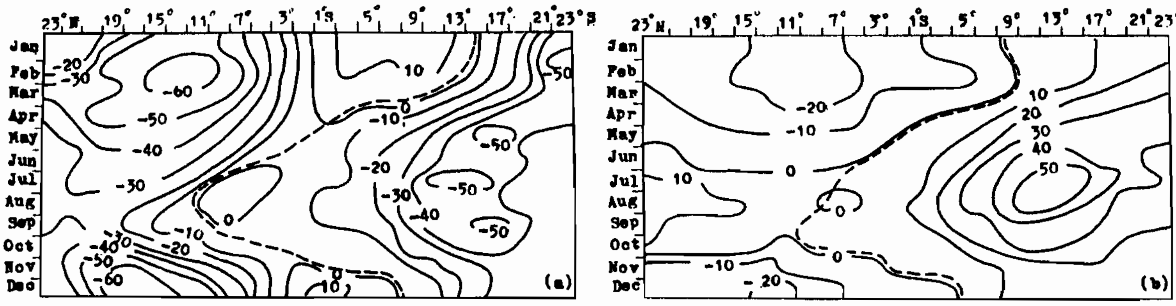

FIG.1. Long-term monthly mean of the zonal (a) and meridional (b) components of the pseudo wind stress along 155°E. (in $m^2.s^{-2}$). The dashed lines are the interface of the opposite wind components.

Monthly mean zonal and meridional wind stresses (τ') can be represented by its first and second harmonic coefficient,

$$\tau' = <\tau> + a_1 \cos \omega_1 t + b_1 \sin \omega_1 t + a_2 \cos \omega_2 t + b_2 \sin \omega_2 t \qquad (2)$$

where a_1, b_1 and a_2, b_2 are the first and second harmonic coefficients, respectively, $\omega_1=2\pi/12$, $\omega 2=2\pi/6$, t is the time in month, and $<\tau>$ denotes the annual mean value of the pseudo wind stress components. The harmonic coefficients together with the standard error of estimate (σ) and ratio of amplitude (s6/s12) of the pseudo wind stress in the latitude bands of 0°-4°N and 8°-12°N along 155°E are shown in table 1 where σ, s6 and s12 are defined as:

$$\sigma = [(1/12) \sum_{1}^{12} (\tau_t^1 - \tau_t)^2]^{1/2} \qquad (3)$$

$$s6 = (a_2^2+b_2^2)^{1/2} \qquad s12 = (a_1^2+b_1^2)^{1/2} \qquad (4)$$

here τ_t are the monthly mean values of the pseudo wind stress components.

		a1	b1	a2	b2	σ	s6/s12	$<\tau>$
0°-4°N	τ^x	- 3.3	- 5.2	0.7	-4.0	0.5	0.67	- 6.4
	τ^y	- 8.6	- 4.0	-2.3	-0.8	4.9	0.26	- 1.3
0°-8°N	τ^x	-22.7	-17.1	-1.5	5.3	11.7	0.19	-35.4
	τ^y	-14.7	- 8.2	-1.7	-0.4	12.1	0.11	-10.5

Table 1. Harmonic coefficients (a_1, a_2, b_1, b_2), σ and s6/s12 of the pseudo wind stress along 155°E (see text for definition).

The standard errors (σ) are smaller than the largest harmonic coefficient in both latitude bands. The ratios of the second to the first harmonic amplitudes (s6/s12) in the 0°-4°N band are not negligible, particular for τ^x. It shows that the semiannual variation is apparently near the equator.

Fig. 2 represents the seasonal variations of the zonal pseudo wind stress (τ^x) as calculated from equation (2). Near the equator (Fig.2a), the surface wind has apparent semiannual variation. When the ITCZ shifts across 2°N during May to June and October to November, it causes a decrease of the easterly wind. But near 10°N there is a marked anuual cycle (Fig. 2b), because the ITCZ arrives nearly 10°N once a year.

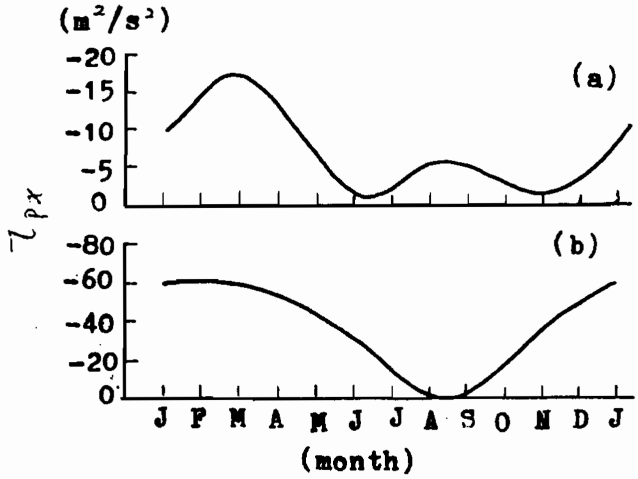

FIG.2. Seasonal variation of zonal pseudo wind stress calculated from harmonic coefficients at 2°N 155°E (a) and 10°N 155°E (b).

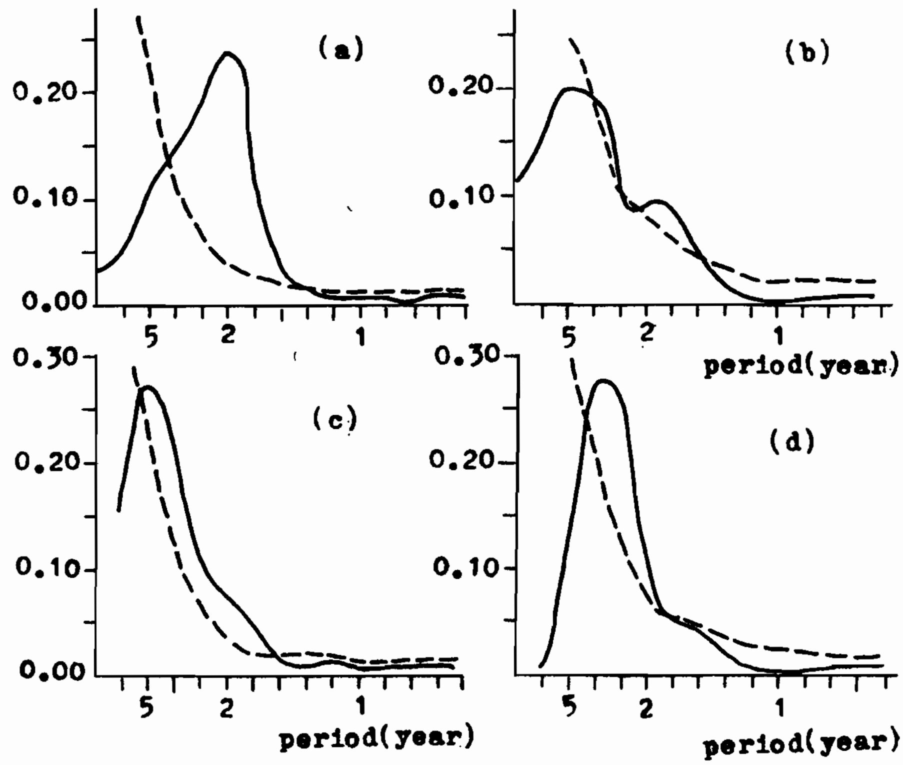

FIG.3. Power spectra of monthly anomalies of the zonal pseudo wind stress for four latitude bands, along 155°E. The dashed lines are confidence limit of 95% red noise.

b. Interannual variations.

Power spectrum of monthly anomalies of the zonal pseudo wind stress (τ^x) for four latitude bands (0°-10°S, 10°-20°S, 0°-10°N and 10°-20°N) along 155°E are displayed in Fig.3. These spectra curves have a marked peak at 2-4 year period, it indicates that the zonal wind over the western tropical Pacific has a main 2-4 year period of variation, corresponding to that of ENSO events.

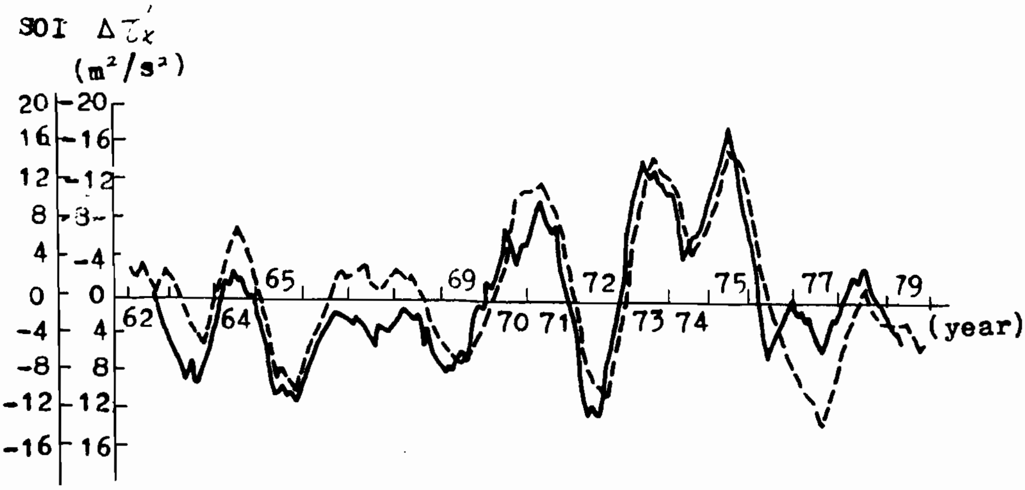

FIG.4. Time series of the average zonal pseudo wind stress anomalies over 3°N-3°S; 140°E-170°W (solid line) and Southern Oscillation Index (dashed line). Both curves have been smoothed with an 11-month running mean.

The solid line in Fig.4 is the time series of the zonal pseudo wind stress anomalies over 3°S-3°N and 140°E-170°W ($\pm3°\Delta\tau^x$). The curve shows that there is a strong westerly wind anomaly ($>5m^2.s^{-2}$) during ENSO years. The dotted line in Fig.4 is the time series of the Southern Oscillation Index (SOI, taken from Parker (1983). Wind anomalies ($\Delta\tau^x$) over ±3° area closely related to SOI. The monthly correlation coefficient of these two time series is -.87.

c. Surface windfield anomalies during the ENSO period.

The time-longitude section of the composite monthly zonal wind stress anomalies along the equator for four El Nino years (1965, 1969, 1972, 1976) is shown in Fig.5. The composite span 36 months beginning 12 months before and ending 12 months after a given El Nino year. Fig.5 shows anomalous variations of the surface wind field in the period of ENSO event. Several months prior El Nino years, easterly winds are stronger than normal, but in October to November preceding El Nino years, westerly wind anomalies replaced easterly wind anomalies over the western edge of the tropical Pacific, migrating eastward gradually. During March to April of El Nino years the westerly anomalies covered all area of the western equatorial Pacific and the magnitude can be above 20 $m^2.s^{-2}$. At the end of El Nino years, easterly wind anomalies are present again.

The time-latitude section of the difference between τ^x for four El Nino years (1965, 1969, 1972, 1976) and that of the long term monthly mean (1964-1980) along 155°E, is displayed in Fig.6. From Fig.6 it is apparent that during El Nino year westerly wind anomalies are prevailing over the western tropical Pacific, particularly in the 10°S-10°N. band. There are two periods in which westerly wind anomalies strengthen, one is in the northern hemisphere during February to April, and the other is in the southern hemisphere during August to October.

3. Effects of the wind field on upper ocean thermal structure

a. Effect of the wind stress curl on the depth of thermocline.

Meyers (1975) used the following formula to approximately estimate the seasonal variation of the depth of 14°C isotherm

$$W_b = \nabla \times (\tau/\rho f) + \nabla . M_g \qquad (5)$$

where τ is the wind stress vector, f the coriolis parameter, ρ the density of the mixed layer, ∇M_g the vector of horizontal geostrophic transport in the layer between the surface and depth B, and W_b the vertical velocity at depth B. Donguy et al. (1982) used Eq.5 and estimated and analyzed the seasonal and interannual variations of the depth of the thermocline in the central tropical Pacific.

In our case, for lack of long-term salinity data, the term of the divergence of geostrophic transport ($\nabla . M_g$) is neglected. Since $\tau^y{}_x$ is much smaller than $\tau^x{}_y$ (see Table 2.) except at 16°N, during April to May, where both are small, equation (5) can be reduced to:

$$Wb = -(\tau^x/\rho f)_y \qquad (6)$$

According to long-term monthly mean (1964-1980) τ^x, one can estimate the seasonal variations of the depth of the thermocline. The integrated curves of W_b calculated by equation (6) are shown in Fig.7. At 8°N-155°E, the thermocline depth displays semiannual variations that can be explained by seasonal oscillations of the position of the ITCZ. In September-October, the ITCZ is situated in the 8°N band. Therefore, zonal wind stress and its curl near 8°N are weaker than annual mean values. The thermocline (or the isotherm in upper layer) descends from annual mean depth, responding to weaker Ekman pumping. During June to July and November to December, the ITCZ is south of 8°N, so the wind stress curl at 8°N is stronger than the annual mean, the thermocline (also the isotherm line) is rising in response to stronger Ekman pumping. In March the ITCZ is at its southernmost position (near 15°S), northeast trade are strong but uniform near 8°N. So the thermocline descends in response to weaker wind stress curl. Because sea level and thermocline depth are 180° out of phase in the equatorial ocean, sea level data taken at station near the equator permit a test of the analyzed thermocline (also isotherm depth in upper layer ocean). The dashed line in Fig.7 is Truk island (7°28'N, 151°51'E) monthly mean sea level (after Meyers, 1982). It shows 180° out of phase with the solid line (computed curve). The dotted line in Fig.7 is observed long-term mean (1964-1974) seasonal variations of the 20°C isotherm depth, which is similar to the computed curve.

		1	2	3	4	5	6
8°N	$\tau^x{}_y$	14.2	13.8	7.2	19.3	15.3	14.9
	$\tau^y{}_x$	2.6	0.9	2.8	0.7	1.5	0.7
16°N	$\tau^x{}_y$	17.1	13.1	25.2	1.1	0.0	4.4
	$\tau^y{}_x$	1.8	1.3	1.5	0.7	1.1	0.2

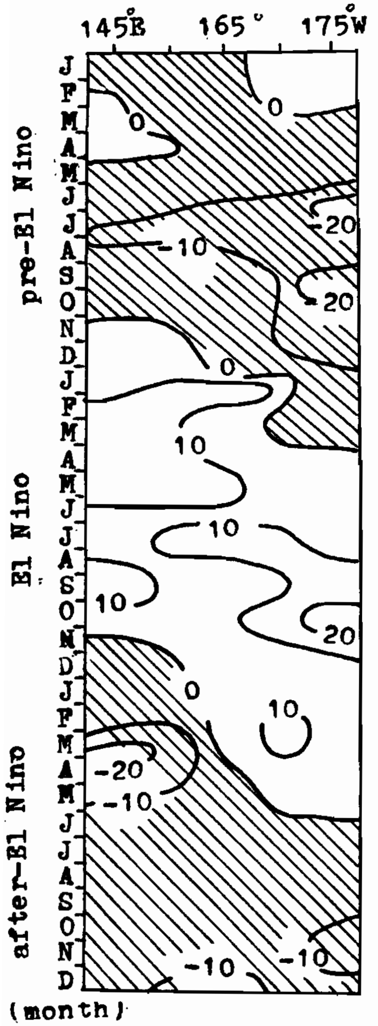

FIG.5. Time-longitude section of composite monthly zonal pseudo wind stress anomalies (in $m^2.s^{-2}$) along the equator for four El Nino years (1965, 1969, 1972, 1976). Shaded areas indicate east wind anomalies.

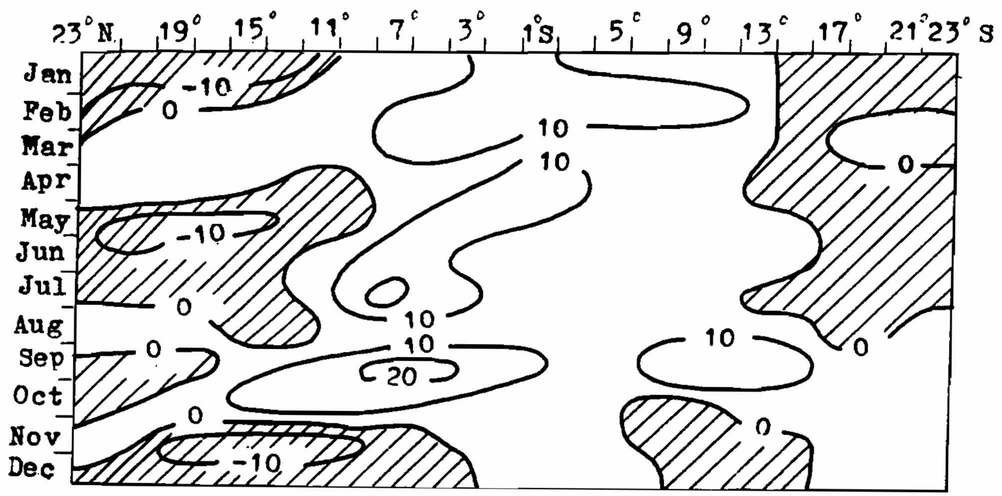

FIG.6. Time-latitude section of the difference between the monthly mean (zonal pseudo wind stress) for four El Nino years (1965, 1969, 1972 and 1976) and that of long term (1964-1980) monthly mean.

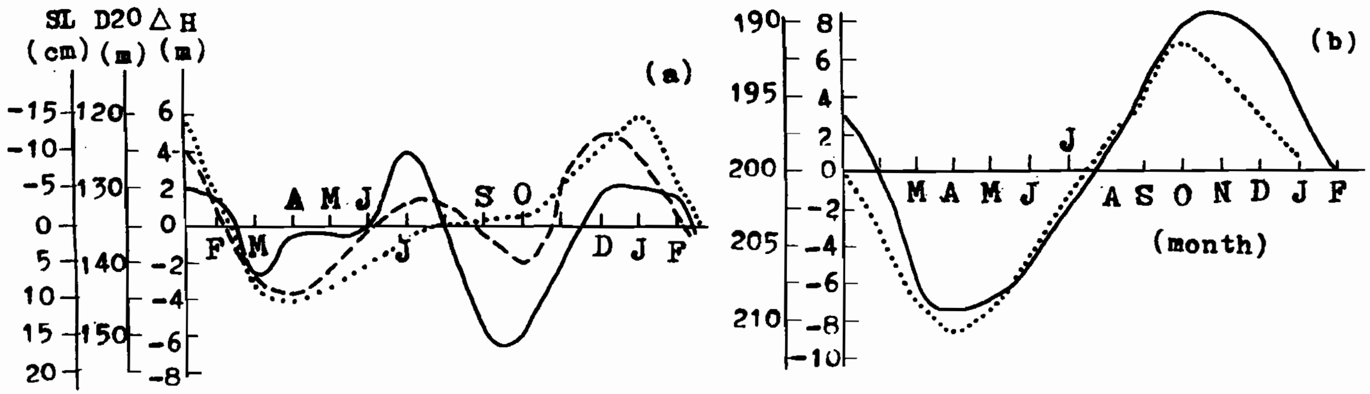

FIG.7. Seasonal variation of the thermocline depth at (a) at 8°N-155°E, (b) 16°N-155°E, as calculated by equation 6 (solid line). The dotted line denotes the long-term mean depth of the 20°C isotherm. The dashed line denotes the long-term mean sea level at Truk Island (7°28'N- 151°51'E), after Meyers (1982).

		7	8	9	10	11	12
8°N	τ^x_y	21.9	6.1	3.1	5.9	20.8	24.1
	τ^y_x	0.2	0.7	0.0	0.0	1.1	1.5
16°N	τ^x_y	7.2	10.5	12.0	14.2	2.2	3.9
	τ^y_x	0.4	2.2	0.4	0.2	1.3	0.0

Table 2. Monthly mean value of τ^x_y and τ^y_x at 8°N-155°E and 16°N-155°E (in cm.day^{-1})

At 16°N-155°E, both computed and observed thermocline depth have only one cycle per year (Fig.7b). During September to October the ITCZ reaches its northeast position, and at 16°N the wind stress curl is stronger: isotherms rise in response to the stronger Ekman pumping. In March, the ITCZ reaching its at the southeasternmost position, wind stress curl is weaker at 16°N due to uniform wind field, and the isotherms descend.

As described above, the effects of Ekman pumping produced by wind stress curl on the upper ocean thermal structure are visible. It can explained mean seasonal variations of the thermocline depth in the Western Tropical Pacific.

b. Effect of zonal wind stress on the Western Pacific Warm Pool.

In this section seasonal wind stress anomalies $\Delta\tau^x$ computed over ±3° area (defined as in section 2), represent variations of zonal wind stress in the western equatorial Pacific. We use the number of grid points at which the mean temperature from sea surface to 100m depth are warmer or equal to 28°C (west of 180° and north of the equator), to represent the volume of the Western Pacific Warm Pool (the T28 time series was taken from Lin, 1989). Its variations appear to be related to the equatorial zonal wind stress. The correlation coefficient of these two seasonal mean time series is -0.70 (n=52 seasons).

c. Relationship between zonal wind stress and other thermal indexes of the western tropical Pacific.

As indicated in Katz et al (1977), it is generally assumed in theoretical work that the vertically integrated zonal pressure gradient (in the upper ocean) can be equated to the zonal component of the wind stress. After analyzing the GATE's data, they showed strong correlation between zonal pressure gradient and simultaneously observed zonal wind stress. Donguy et al (1984) use zonal slope of thermocline to represent the zonal pressure gradient, and analyze its relation to zonal wind stress in the central Pacific. In the present study, zonal slope of the 20°C isotherm between 140°E and 180° in the 3°N-3°S band (D20), from 1964-1974, is calculated. D20 seasonal time series appear to be related to zonal wind stress anomalies (as calculated above), the correlation coefficient between the two series is -0.52 (n=38 seasons).

We also use seasonal difference of the 20°C isotherm depth between 7.5°N and 2.5°N, along 155°E, to indicate the strength of the NECC. We define T27 as T28 except for mean temperature higher or equal to 27°C, to indicate the mixed layer heat content in the western tropical Pacific. All of these upper ocean thermal indexes are related to the wind field. Their cross correlation coefficients are shown in table 3. From table 3, it is apparent that the sea surface wind field over the western equatorial Pacific plays an important role in changing the upper layer ocean thermal structure.

$(\pm 3^\circ \Delta\tau^x$	-.86*	-.45	-.52*	-.58*	-.70
	(62,0)	(31,1)	(38,1)	(52,0)	(52,0)
T28	-.70*	-.56*	.43	.83	
	(52,0)	(31.0)	(38,0)	(52,0)	
T27	-.62*	-.62*	.51*		
	(38,0)	(31,0)	(38,0)		
D20	-.37	-.14			
	(38,0)	(30,0)			
NECC	-.21				
	(30,0)				

Table 3. Cross correlation coefficients between the wind field and the upper ocean thermal indexes (numbers in parentheses are the seasons of time series and lag). Stars denote significance at the 1% level.

4. Conclusion

The primary results of the present study are:

(1) The surface wind field over the western tropical Pacific have apparent annual cycle. Near the equator, it has apparent semiannual variations, because the ITCZ crosses the equator twice a year.

(2) The interannual variations of the surface wind field over the western tropical Pacific present a main variation of 2-4 years, consistent with that of the ENSO event. The zonal wind over the western equatorial Pacific is closely related to SOI (correlation coefficient is -0.87).

(3) In the western tropical Pacific mean seasonal variations of the thermocline depth, and of sea level near the equator can be explained by displacement of the surface wind field (indicated by the ITCZ position).

(4) From correlation analysis of long-term historical data, it is apparent that the sea surface wind field over the western equatorial Pacific plays an important role in changing the upper layer thermal structure of the ocean.

The data sets used in this study have poor resolution but the interannual variations of the wind field and the thermal structure are strongly related to ENSO events. Therefore some primary results can be obtained as above. More complete data sets are necessary to analyze more details. Wind field and upper ocean thermal structure data sets will be greatly improve within the international TOGA programme.

REFERENCES

Donguy, J.R. and C. Hénin, 1981: Two types of hydroclimatic conditions in the south-western Pacific. *Ocean. Acta*, **4**, 57-62.

Donguy, J.R., C. Hénin, A. Morliere and J.P. Rébert, 1982: Thermal changes in the western tropical Pacific in relation to the wind field, *Deep-sea Res.*, **29**, 869-882.
Donguy, J.R., A. Dessier, G. Eldin, A. Morliere and G. Meyers, 1984: Wind and thermal conditions along the equatorial Pacific. *J. Mar. Res.*, **42**, 103-121.
Katz, E.J. and Collaborators, 1977: Zonal pressure gradient along the equatorial Atlantic. *J. Mar. Res.*, **35**, 293-307.
Lin Chuanlan, 1989: Some features of the heat content changes of the ocean upper layer in the Northwest Pacific during period 1964-1982. Submitted to Tropical ocean. (in Chinese)
Meyers, G., 1975: Seasonal variation in transport of the Pacific North Equatorial Current relative to the wind field. *J. Phys. Oceanogr.*, **5**, 442-449.
Meyers, G., 1982: Interannual variation in sea level near Truk Island: a bimodal seasonal cycle. *J. Phys. Oceanogr.*, **12**, 1161-1168.
Parker, D.E., 1983: Documentation of a Southern Oscillation Index. *Meteoro. Mag.*, **112**, 184-188.
White, E.B., G. Meyers, J.R. Donguy and S.E. Pazan, 1985: Short-term climate variability in the thermal structure of the Pacific Ocean during 1979-1982, *J. Phys. Oceanogr.*, **15**, 917-935.
Wyrtki, K., 1974: Equatorial current in the Pacific 1950-1970 and their relations of the trade wind. *J. Phys. Oceanogr.*, **4**, 372-380.

WESTERN PACIFIC INTERNATIONAL MEETING AND WORKSHOP ON TOGA COARE

Nouméa, New Caledonia
May 24-30, 1989

PROCEEDINGS

edited by

Joël Picaut *
Roger Lukas **
Thierry Delcroix *

* ORSTOM, Nouméa, New Caledonia
** JIMAR, University of Hawaii, U.S.A.

INSTITUT FRANÇAIS DE RECHERCHE SCIENTIFIQUE
POUR LE DÉVELOPPEMENT EN COOPÉRATION

ORSTOM

Centre de Nouméa

TABLE OF CONTENTS

MEETING COLLECTED PAPERS

WATER MASSES, SEA SURFACE TOPOGRAPHY, AND CIRCULATION

EL NINO/SOUTHERN OSCILLATION 1986-87

MOMENTUM, HEAT, AND MOISTURE FLUXES BETWEEN ATMOSPHERE AND OCEAN

EMPIRICAL STUDIES OF ENSO AND SHORT-TERM CLIMATE VARIABILITY